ISSN 1846-6168 (Print), ISSN 1848-5588 (Online)
https://doi.org/10.31803/tg-20240423182840

Subject review
Received: 2024-04-23, Accepted: 2024-04-30

Development of Guidelines for the Design of Cantilevers

Filip Šulentić, Daniel Miler, Matija Hoić*

Abstract: Cantilevers are elements typically used in the design of various structures such as factory halls or cantilever cranes. Traditionally, such elements are made of standard profiles or, in the case of large loads, by welding from standard sheets. Often, due to stationary conditions of exploitation, no attention is paid to mass reduction. Increasingly stringent requirements on reducing costs, but also on reducing environmental impact through reducing energy consumption necessary for the production, processing, and transport of materials, facilitate the application of optimization to obtain a construction solution with minimal mass. However, doing so requires advanced high-cost computer tools and increases the required competencies of designers. In this paper, a series of optimizations have been carried out for typical reach and load values of cantilevers aiming to create a database that will facilitate algorithms for selecting cross-sectional dimensions suitable for production using either additive technologies or traditional methods.

Keywords: cantilever; deflection; guidelines; optimization; strength

1 INTRODUCTION

Cantilevers are a common structural element in a range of applications, from common load-bearing structures to energy sources where they convert mechanical vibrations into electrical energy through the piezoelectric effect [1]. The development and application of optimization methods therefore did not bypass even this simple structural element. Newer studies cover a wide range of applied methods, which include the use of neural networks to search for the optimal design [2], topological optimization by subtracting material to achieve the smallest mass [3], and heuristic methods such as simulated annealing [4].

In specific cases, cantilevers have a complex design, that includes active components, so the active control of the deformation of the cantilevers is achieved through the application of dielectric elastomers [5], the application of piezoelectric layers aims to actively manage the vibration modes of the cantilever [6], and the design of composite versions is also being improved [7]. The calculation of large deformations of both simple [8] and multi-stage cantilevers [9] is also investigated.

Advanced methods enable obtaining innovative results; however, for most applications in everyday engineering practice, they may not necessarily be applicable. This is because they require the application of advanced knowledge, and the use of expensive computer programs to solve typical recurring problems. An alternative approach is the formation of design guidelines based on statistical analysis of optimized solutions for a wide range of design parameters for the observed mechanical system.

In this article, an example of a console as a load-bearing element in load-bearing structures is considered. Chapter 2 describes the general engineering problem of designing a load-bearing cantilever with a constant rectangular section. In the third chapter, the application of the parametric optimization module in the Ansys software package is described. Further, optimization results are analysed in Chapter 4, and the guideline formation process is described. The discussion, main conclusions, and possibilities for further development are given in the final chapter.

2 CANTILEVER DESIGN

The cantilever under consideration is a simple structure with a constant rectangular cross-section. The console is fixed at one end, loaded with a concentrated force at the other end and by its mass (Fig. 1a). The section of the console (Fig. 1b) consists of two identical vertical bands of width t and height h and two identical horizontal bands of width b and height t. Vertical bands are spaced at distances equalling $0{,}8b$ as this distance relates to typical classic welded steel sheet design. Moreover, the same design could also be used if manufactured using one of the more recently emerging technologies such as additive manufacturing. The target material is a typical structural steel such as S235.

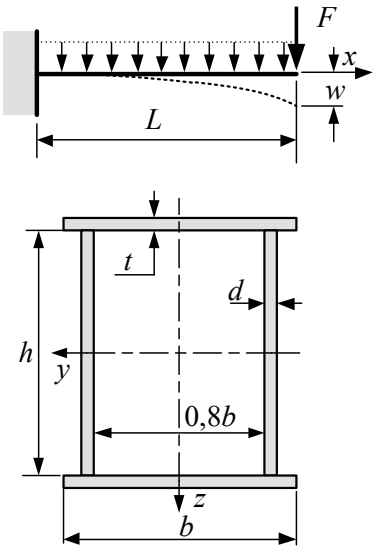

Figure 1 Cantilever beam model (top) and its cross-section (bottom)

The set of typical values of reach L and concentrated loads F are as follows: $L = \{2, 4, 6, 8\}$ m and $F = \{1, 2, 3, 5\}$ kN. The permissible deflection of the console was set to $w = L/600$, while the permissible stress was taken as $\sigma = 120$ MPa.

3 OPTIMIZATION PROCEDURE

The optimisation was carried out using a parametric optimization module within *Ansys* based on an Adaptive Single-Objective The selected method utilizes a gradient-based algorithm, thus yielding a refined, global optimum. The method is applicable to single-objective problems with multiple constraints and aims to find the global optimum. It is limited to continuous and manufacturable input parameters.

Firstly, the CAD model is designed with nominal values of individual dimension (Fig. 2a), fixed at one end (Fig. 2b), and continous force uniformly distributed across the opposite cross-section (Fig. 2c).

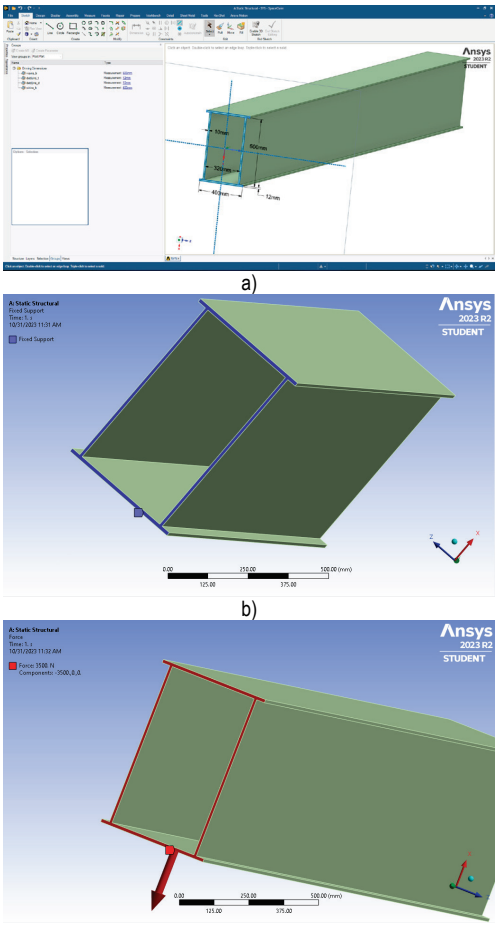

Figure 2 FEM analysis setup within Ansys

Optimization of initial design is conducted through variation of dimension values of the initial design. Upper and lower boundary for each of four dimensions are set at approx. 90 and 110 % of the initial values (Fig. 3).

Optimization problem goal was minimizing the overall mass of the cantilever while adhering to the requirements regarding the maximum allowable deformation and stress (Fig. 4).

The optimization process was started, and the initial FEM analysis is conducted using cubic elements, providing results on stress and deformation (Fig. 5).

Table of Schematic B2: Optimization

	A	B	C	D
1	Input Parameters			
2	Name	Lower Bound	Upper Bound	
3	P1 - visina_h (mm)	500	700	
4	P2 - debljina_t (mm)	10	14	
5	P3 - debljina_d (mm)	8	12	
6	P4 - sirina_b (mm)	320	480	
7	Parameter Relationships			
8	Name	Left Expression	Operator	Right Expression
*	New Parameter Relationship	New Expression	<=	New Expression

Figure 3 Lower and upper boundaries of design variables

Table of Schematic B2: Optimization

	A	B	C	D	E	F	G	H	I
1	Name	Parameter	Objective			Constraint			
2			Type	Target	Tolerance	Type	Lower Bound	Upper Bound	Tolerance
3	P5 <= 13.3 mm	P5 - Total Deformation Maximum	No Objective			Values <= Upper Bound		13.3	0.001
4	P6 <= 120 MPa	P6 - Equivalent Stress Maximum	No Objective			Values <= Upper Bound		120	0.001
5	Minimize P7	P7 - Geometry Mass	Minimize	0		No Constraint			
*		Select a Parameter							

Figure 4 Optimization problem setup

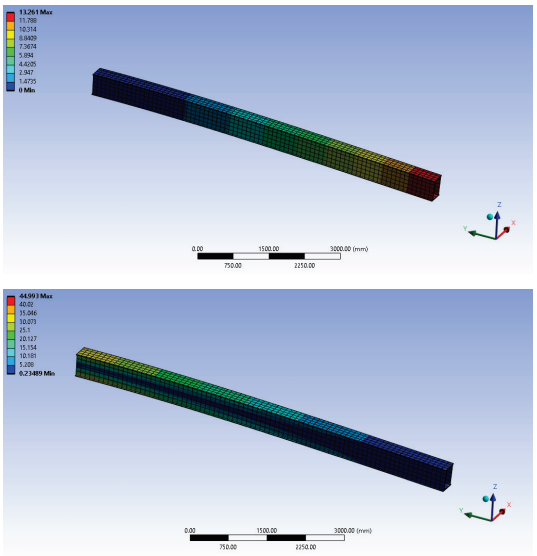

Figure 5 FEM analysis results for L = 8 m, F = 5 kN

If the initial design results in satisfactory stress and deformation, or stress and deformation results that are slightly above target values, the optimization module will generate several additional candidates and repeat the FEM analysis for each candidate. Based on the results of the newly generated solutions, the program generates the subsequent candidates by combining somewhat altered dimensions of the current generation (Fig. 6).

Table of Schematic B2: Optimization

	A	B	C	D	E	F	G	H
1	Name	P5 - h (mm)	P6 - h (mm)	P7 - t (mm)	P8 - d (mm)	P9 - Total Deformation Maximum (mm)	P10 - Equivalent Stress Maximum (MPa)	P11 - Geometry Mass (kg)
4	3	DP 14	335.62	516.09	10.078	12.364		
5	4		373.86	475.04	10.188	11.932		
6	5	DP 16	361.11	545.42	9.4209	11.357		
7	6		395.1	510.23	9.5305	11.645		
8	7		327.12	469.18	9.0923	12.22		
9	8		365.36	451.58	9.3114	11.501		
10	9		348.36	463.31	9.8591	13.083		
11	10		356.86	504.36	8.5446	11.214		
12	11		386.6	498.5	9.64	13.226		
13	12	DP 23	369.61	539.55	9.9687	12.508		
14	13	DP 24	344.12	521.96	9.2019	13.37		
15	14		339.87	492.64	9.7496	11.07		
16	15	DP 26	331.37	527.82	8.8732	12.076		
17	16		390.85	480.91	8.6541	11.789		
18	17	DP 28	382.35	533.69	8.7637	12.651		

Figure 6 Generation of further potential optimal solutions

By variation of dimensions for successful solutions, the procedure results in improved solutions which tend to approach an optimum. Once the improvement in mass reduction is no longer significant, the procedure stops

resulting in a solution that is very near to the optimal one (Fig. 7).

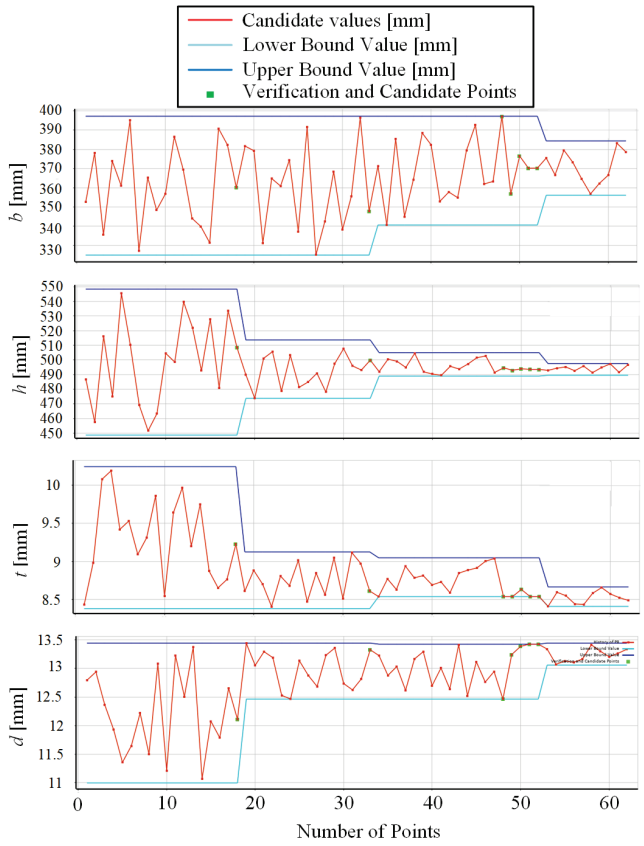

Figure 7 Generation of further potential optimal solutions

It should be noted that the choice of upper and lower boundaries might prevent the algorithm in finding either feasible (if the upper dimension values are too small to achieve acceptable stress and/or deformation) or optimal solution (if the lower boundaries results in stress and/or deformation which are well above set limits). One solution would be to widen the boundaries. However, wider boundaries will induce a wide variation in potential solutions, prolonging the optimization process. This, on the other hand, may significantly increase optimization times for individual set of parameters to several hours, possibly even hindering the ability to find optimum solution. The choice of initial solution and boundary width thus have a significant impact on the overall required time.

Additionally, the size of the finite elements was set automatically, i.e. the mesh density may not be sufficient to result in a realistic stiffness and consequently stress values. More then 60 FEM analysis was conducted per each optimization which resulted in several hours of computing per each of 18 investigated combinations using a moderate power personal computer. Mesh with higher density would thus necessitate usage of workstation grade computer which was not available in this case.

Herein, the procedure was started by finding optimal solution for the greatest force and reach. Several attempts were needed until a good set of initial parameters and boundary widths was found. Once the optimal solution was found for this extreme case, optimization was conducted for neighbouring sets of loads and reach with initial sets of dimensions being set as approx. 10 % lower than the optimum solution for the extreme case. The same approach was then used for each subsequent set of smaller loads and reaches.

As the algorithm progresses, it might find that the limits are narrowed down, and it will do so dynamically to speed up the process (blue and light blue lines in Fig. 7). For each combination of load, reach, initial dimensions, and boundaries, properly set limits will result in the optimum solution being within boundaries. Further, it may be observed that the algorithm will widen the limits from their contracted values if needed; however, not beyond limits initially set by the user.

Once the improvement in the obtained solutions falls under the set limit, the program will stop and offer the three best solutions, i.e. three solutions with the smallest overall masses. Herein, the solution with the smallest mass of three is selected for further analysis.

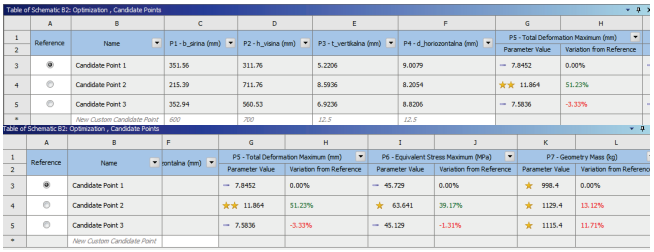

Figure 8 Example of three offered solutions after the termination of optimization procedure

4 ANALYSES OF RESULTS

A total of 18 combinations were investigated for the target range of loads and reaches with basic 16 combinations made from four values for force and lever length and two additional outlying sets which include smaller force and longer reach and vice versa. The results are presented in Tab. 1 and Fig. 9.

Table 1 Overview of obtained solutions

	F	*L*	*b*	*h*	*t*	*d*
1	5	8000	333,6	450,1	8,4	10,9
2	3	8000	308,2	433,7	8,2	10,1
3	5	6000	310,9	406,2	8,8	10,6
4	3	6000	259,7	413,4	7,9	9,2
5	2	8000	248,7	364,2	7,6	8,9
6	5	4000	269,9	337,8	7,4	8,6
7	3	4000	207,1	264,0	6,9	7,6
8	2	4000	177,2	224,4	7,0	8,4
9	5	2000	183,0	288,0	6,2	6,5
10	2	6000	182,4	284,7	6,8	7,7
11	1	6000	151,9	302,1	6,3	6,7
12	1	8000	199,4	304,1	7,2	8,3
13	1	4000	125,3	277,3	5,2	5,1
14	3	2000	93,7	183,5	5,0	6,1
15	2	2000	79,8	150,3	3,2	4,5
16	1	2000	62,3	153,5	3,1	4,4
17	5	9000	375,5	492,8	8,4	13,3
18	0,5	1000	74,2	155,2	4,1	4,6

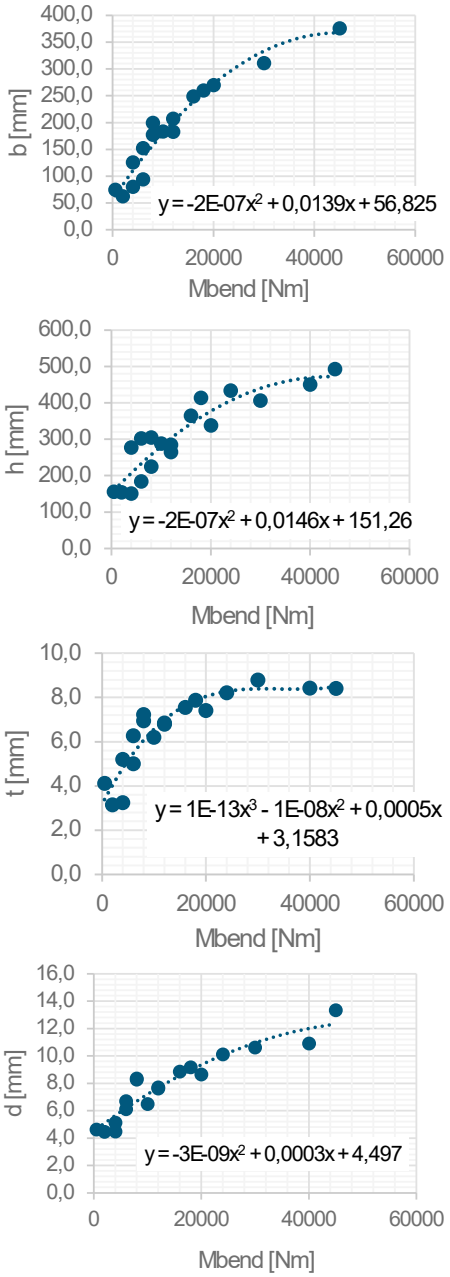

Figure 9 Example of three offered solutions after the termination of the optimization procedure

Obtained optimal dimensions for a given combinations of loads and reaches are plotted in Fig. 9 where x-axis shows the bending torque calculated as $M_{bend} = F \cdot L$, and the y-axis shows corresponding dimension values. It may be observed that the results can be described well using a 2nd or a 3rd order polynomial. The $y = f(x)$ equations shown in the figures thus allow the user to calculate the near optimum dimensions of the cantilever cross section for the known required reach and concentrated load at that reach.

Some variations in Fig. 9 can be observed with several points of optimum solutions being quite far from the regression curve. Hence, further analysis of stress and deformation were carried out as the obtained values from FEM analysis were used as limits during optimization. Analytical equations were used to obtain stress and deformation values for the obtained optimal solutions [10]:

$$w = \frac{FL^3}{3EI} + \frac{qL^4}{8EI}, \tag{1}$$

$$\sigma = \frac{FL}{W} + \frac{qL^2}{2W}, \tag{2}$$

where the cross-section characteristics are as follows:

$$I_y = 2\left[\frac{dh^3}{12} + \frac{bt^3}{12} + \left(\frac{h+2t}{2}\right)^2 tb\right], \tag{3}$$

$$W_y = \frac{I_y}{2(h+2t)}. \tag{4}$$

Furthermore, continuous load due to the cantilever weight is:

$$q = g \cdot A \cdot \rho, \tag{5}$$

where g = 9.81 N/s^2, A is the cantilever cross-section area, and ρ = 7850 kg/m^3 is the density of steel.

Comparison of results is given in Tab. 2 and Fig. 10. Obtained results have shown that both deformations and stresses were lower for numerical solutions compared to results obtained via analytical equations. It is reasoned that this is a result of the high stiffness of the FEM model, indicating that the mesh density should be increased.

Table 2 Comparison of stress and deformation obtained for optimum solutions using FEM (σ_{op}, w_{op}) and analytical equations (σ_{an}, w_{an})

	σ_{op}	w_{op}	σ_{an}	w_{an}
1	44,99	13,26	23,33	8,92
2	30,92	12,70	20,01	11,67
3	26,87	9,56	17,17	5,54
4	46,02	10,00	15,08	4,96
5	28,33	12,48	22,75	15,90
6	55,68	5,87	15,07	2,42
7	65,65	5,39	16,92	3,50
8	67,07	6,42	16,41	4,06
9	73,23	3,29	12,79	0,56
10	73,05	9,83	22,88	10,70
11	67,26	9,86	17,85	8,36
12	63,37	13,18	23,56	20,34
13	46,49	3,34	13,03	2,75
14	68,02	3,17	26,27	1,79
15	65,00	3,28	37,70	3,15
16	35,55	1,51	23,59	1,99
17	60,91	14,89	24,70	16,03
18	33,62	1,49	4,28	0,09

Correlation factors between numerical and analytical results are 0,88 and 0,23 for deformation and stress, respectively. It may be reasoned that maximum stress is a single value, i.e. a value of a single finite element, which may, particularly in the case of inner angles be unrealistic, i.e. the value may simply refer to the stress concentration rather than realistic value. On the contrary, maximum deformation is a sum of deformations of many individual

elements where a single unrealistic value will have an insignificant effect on the overall value. Again, increasing the mesh density may partially resolve this problem, albeit values that are more realistic may also necessitate redefinition of boundary conditions.

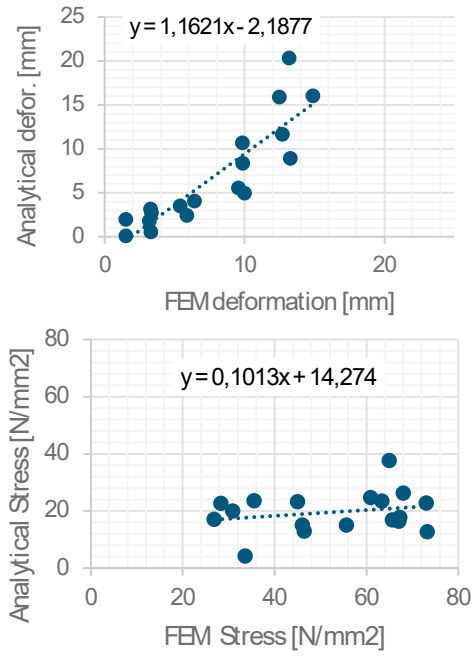

Figure 10 Comparison of deformation and stress using analytical and FEM methods

5 CONCLUSIONS

The paper presents a proposal on the approach of development of guidelines for designing a cantilever for a typical set of parameters occurring in steel structures. The application of Ansys optimization parametric tools facilitated a fast and consistent tool to generate optimum solutions for a wide range of design parameters.

It should be noted that the applied geometry is typically related to the welded steel sheet design, however, similar geometry may be obtained using different technologies including extrusion and additive manufacturing, hence developed guidelines may enable simple straightforward means of designing near optimized cantilever design elements resulting in reduced requirements for material, energy, transportation, and assembly requirements.

Analysis of obtained results, and particularly comparison of numerical and analytical results of calculated stresses and deformation show significant differences. Results point to the conclusion that the numerical analysis should be further developed and detailed to ensure that it provides reliable values. Hence, the guidelines obtained herein are not suitable for general application, and a more detailed procedure for the development of design guidelines should be developed. However, obtained results show that a functional relationship between design requirements consisting of load and reach of the cantilever and values of cross-section dimensions can be defined, i.e. that the proposed approach has merit and that investing additional resources, particularly computational power, should results in obtaining functional guidelines for designing near optimum cantilever design.

6 REFERENCES

[1] Zamanian, M. & Firouzi, B. (2024). Analysis and Optimal Design of Vibration-Based Paddle Type Piezoelectric Energy Harvester Under Electrostatic Actuation. *J. Vib. Eng. Technol*. https://doi.org/10.1007/s42417-024-01280-9

[2] Lew A. J. & Buehler, M. J. (2021). Encoding and exploring latent design space of optimal material structures via a VAE-LSTM model. *Forces in Mechanics, 5*, 100054. https://doi.org/10.1016/j.finmec.2021.100054

[3] Qiu, C., Du, S. & Yang, J. (2021). A deep learning approach for efficient topology optimization based on the element removal strategy. *Materials & Design, 212*, 110179. https://doi.org/10.1016/j.matdes.2021.110179

[4] Rostami Najafabadi, H., Martins, T. C., Tsuzuki, M. S. G. & Barari, A. (2004). Structural Design with Self-Weight and Inertial Loading Using Simulated Annealing for Non-Gradient Topology Optimization. *Machines, 12*(1), 25. https://doi.org/10.3390/machines12010025

[5] Liu, C., Mao, B., Huang, G., Wu, Q., Xie S. & Xu, M. (2018). Optimization of shape control of a cantilever beam using dielectric elastomer actuators. *AIP Advances, 8*(5), 055015. https://doi.org/10.1063/1.5026160

[6] Huang, Z., Huang, F., Wang, X., Chu, F. (2023). Active Vibration Control of Composite Cantilever Beams. *Materials, 16*(1), 95. https://doi.org/10.3390/ma16010095

[7] Singh S., Pflug L., Mergheim J. & Stingl M. (2023). Robust design optimization for enhancing delamination resistance of composites. *Int J Numer Methods Eng, 124*(6), 1381-1404. https://doi.org/10.1002/nme.7168

[8] Cui Y., Hong Y., Khan N. A. & Sulaiman M. (2021). Application of Soft Computing Paradigm to Large Deformation Analysis of Cantilever Beam under Point Load. *Complexity, 2021*, Article ID 2182693. https://doi.org/10.1155/2021/2182693

[9] Sargent, B. S., Ynchausti, C. R., Nelson, T. G. & Howell, L. L. (2022). The Mixed-Body Model: A Method for Predicting Large Deflections in Stepped Cantilever Beams. *ASME. J. Mechanisms Robotics, 14*(4), 041001. https://doi.org/10.1115/1.4053376

[10] Den Hartog, J. P. (2012). *Strength of Materials*. Courier Corporation.

Authors' contacts:

Filip Šulentić
University of Zagreb, Faculty of Mechanical Engineering and Naval Architecture,
Ivana Lučića 5, 10000 Zagreb, Croatia
fs220977@stud.fsb.hr

Daniel Miler, PhD
University of Zagreb, Faculty of Mechanical Engineering and Naval Architecture,
Ivana Lučića 5, 10000 Zagreb, Croatia
daniel.miler@fsb.unizg.hr

Matija Hoić, PhD
(Corresponding author)
University of Zagreb, Faculty of Mechanical Engineering and Naval Architecture,
Ivana Lučića 5, 10000 Zagreb, Croatia
matija.hoic@fsb.unizg.hr